Reproductive Toxicology 34 (2012) 93–100

Contents lists available at SciVerse ScienceDirect

Reproductive Toxicology

journal homepage: www.elsevier.com/locate/reprotox

Increased cellular distribution of vimentin and Ret in the cingulum induced by developmental hypothyroidism in rat offspring maternally exposed to anti-thyroid agents

Hitoshi Fujimoto[a], Gye-Hyeong Woo[a], Kaoru Inoue[a], Katsuhide Igarashi[b], Jun Kanno[b], Masao Hirose[c], Akiyoshi Nishikawa[d], Makoto Shibutani[a,e,*]

[a] Division of Pathology, National Institute of Health Sciences, 1–18–1 Kamiyoga, Setagaya-ku, Tokyo 158-8501, Japan
[b] Division of Molecular Toxicology, National Institute of Health Sciences, 1–18–1 Kamiyoga, Setagaya-ku, Tokyo 158-8501, Japan
[d] Biological Safety Research Center, National Institute of Health Sciences, 1–18–1 Kamiyoga, Setagaya-ku, Tokyo 158-8501, Japan
[c] Food Safety Commission, 5–2–20 Akasaka Park Bld. 22nd Floor, Akasaka, Minato-ku, Tokyo 107-6122, Japan
[e] Laboratory of Veterinary Pathology, Tokyo University of Agriculture and Technology, 3–5–8 Saiwai-cho, Fuchu-shi, Tokyo 183-8509, Japan

ARTICLE INFO

Article history:
Received 4 December 2011
Received in revised form 19 February 2012
Accepted 16 March 2012
Available online 6 April 2012

Keywords:
Developmental hypothyroidism
Cerebral white matter
Vimentin
Ret
Rat

ABSTRACT

To elucidate target molecules of white matter development responding to hypothyroidism, global gene expression profiling of cerebral white matter from male rat offspring was performed after maternal exposure to anti-thyroid agents, 6-propyl-2-thiouracil and methimazole, on postnatal day 20. Genes involved in central nervous system development commonly up- or down-regulated among groups treated with anti-thyroid agents. Immunohistochemical distributions of vimentin, Ret proto-oncogene (Ret), deleted in colorectal cancer protein (DCC), and Claudin11 (Cld11) were examined based on the gene expression profile. Immunoreactive cells for vimentin and Ret in the cingulum, and the immunoreactive intensity of Cld11 and DCC in whole white matter were increased by treatment with anti-thyroid agents. Immunoreactive cells for vimentin and Ret were immature astrocytes and oligodendrocytes, respectively. Thus, immunoreactive cells for vimentin and Ret may be quantitatively measurable targets of developmental hypothyroidism in white matter.

1. Introduction

Thyroid hormones are essential for normal fetal and neonatal brain development, control neuronal and glial proliferation in definitive brain regions and regulate neuronal migration and differentiation [1–3]. In humans, maternal hypothyroxinemia early in pregnancy may adversely affect fetal brain development, and importantly, even mild to moderate hypothyroxinemia may result in suboptimal neurodevelopment [4], thereby increasing the concern of impaired brain development induced by exposure to thyroid hormone-disrupting chemicals in the environment.

Developmental hypothyroidism leads to growth retardation, neurological defects and impaired performance in various behavioral learning actions [5,6]. Rat offspring maternally exposed to anti-thyroid agents, such as 6-propyl-2-thiouracil (PTU) and methimazole (MMI), show impaired brain growth including white matter hypoplasia with decreased axonal myelination and oligodendrocytes, and impairment of neurogenesis, neuronal migration, dendritic arborization and synapse formation [2,7–9]. These types of impaired brain growth are permanent and accompanied by apparent structural and functional abnormalities. However, the molecular mechanism of impaired brain growth is still unclear.

Histological lesion-specific gene expression profiling provides valuable information on the mechanisms underlying lesion development. In previous studies, we established molecular analysis methods for DNA, RNA and proteins in paraffin-embedded small tissue specimens using the organic solvent-based fixative methacarn, with high performance similar to that of unfixed frozen tissue specimens [10–12]. These methods have been used to analyze global gene expression changes in microdissected lesions [13–15].

Abbreviations: CC, corpus callosum; Cld11, claudin 11; CNS, central nervous system; DCC, deleted in colorectal cancer protein; GAPDH, glyceraldehyde 3-phosphate dehydrogenase; GD, gestation day; GDNF, glial cell line-derived neurotrophic factor; GFAP, glial fibrillary acidic protein; MMI, methimazole; OSP, oligodendrocyte specific protein; PCR, polymerase chain reaction; PND, postnatal day; PTU, 6-propyl-2-thiouracil; Ret, Ret proto-oncogene; RT, reverse transcription; v-Maf, v-maf musculoaponeurotic fibrosarcoma oncogene; Zfhx1b, zinc finger homeobox 1b.

* Corresponding author at: Laboratory of Veterinary Pathology, Tokyo University of Agriculture and Technology, 3–5–8 Saiwai-cho, Fuchu-shi, Tokyo 183-8509, Japan. Tel.: +81 42 367 5874; fax: +81 42 367 5771.
E-mail address: mshibuta@cc.tuat.ac.jp (M. Shibutani).

0890-6238/$ – see front matter © 2012 Elsevier Inc. All rights reserved.
http://dx.doi.org/10.1016/j.reprotox.2012.03.005

To evaluate in vivo developmental brain growth effects of thyroid hormone-disrupting chemicals, we morphometrically analyzed neuronal migration and white matter development in a rat developmental hypothyroidism model [16]. Molecules involved in aberrant neurogenesis and neuronal mismigration were identified by global gene expression analysis of the hippocampal area [15]. In the present study, to elucidate marker molecules in white matter involved in developmental hypothyroidism, we performed global gene expression profiling using microarrays. To obtain the white matter-specific gene expression profile, a microdissection technique was applied to the corpus callosum (CC) and bilateral cerebral white matter. Based on expression profiles, cellular localization of selected molecules was then immunohistochemically examined in cerebral white matter after developmental exposure to anti-thyroid agents.

2. Materials and methods

2.1. Chemicals and animals

6-propyl-2-thiouracil (PTU; CAS No. 51-52-9) and methimazole (MMI; CAS No. 60-56-0) were purchased from Sigma Chemical Co. (St. Louis, MO). Pregnant CD® (SD) IGS rats at gestational day (GD) 3 (GD 0: the day vaginal plugs appeared) were purchased from Charles River Japan Inc. (Yokohama, Japan). Animals were individually housed in polycarbonate cages (SK-Clean, 41.5 cm × 26 cm × 17.5 cm; CLEA Japan Inc., Tokyo, Japan) with wood chip bedding (Sankyo Lab Service Corp., Tokyo, Japan) and maintained in a climate-controlled animal room (24 ± 1 °C, relative humidity: 55 ± 5%) with a 12 h light/dark cycle. A soy-free diet (Oriental Yeast Co. Ltd., Tokyo, Japan) was chosen as the basal diet for maternal animals to eliminate possible phytoestrogen effects [17]. Animals received food and water ad libitum throughout experimentation including a 1 week acclimation period.

2.2. Experimental design

Animal experiments are described elsewhere [16]. Briefly, maternal animals were randomly divided into four groups including an untreated control. Eight dams per group were treated with 3 or 12 ppm PTU or 200 ppm MMI, which was added to drinking water from GD 10 to postnatal day (PND) 20 (PND 0: the day of delivery). On PND 2, four male and four female offspring per dam were randomly selected and remaining litters were culled. On PND 20, 20 male and 20 female offspring (at least one male and one female per dam) per group were subjected to prepubertal necropsy [16,18]. All animals were weighed and sacrificed by exsanguination from the abdominal aorta under deep anesthesia with ether. Animal protocols were reviewed and approved by the Animal Care and Use Committee of the National Institute of Health Sciences, Japan.

2.3. Preparation of tissue specimens and microdissection

For microarray and real-time reverse transcription (RT)-polymerase chain reaction (PCR) analyses, the whole brain of male offspring was immediately removed at prepubertal necropsy on PND 20 (n = 4/group) and fixed with methacarn solution for 2 h at 4 °C [10]. Coronal brain slices taken at −3.5 mm from the bregma were dehydrated and embedded in paraffin. Embedded tissues were stored at 4 °C until tissue sectioning for microdissection [19].

For microdissection, 4 and 20 μm-thick serial sections were prepared. The 4 μm-thick sections were stained with hematoxylin and eosin for confirmation of anatomical orientation of the hippocampal substructure to aid microdissection (Fig. 1). The 20 μm-thick sections were mounted onto PEN-foil film (Leica Microsystems GmbH, Welzlar, Germany) overlaid on glass slides, dried in an incubator overnight at 37 °C, and then stained using an LCM staining kit (Ambion, Inc., Austin, TX). Regions of CC and bilateral cerebral white matter (external capsule) in sections, as shown in Fig. 1, were subjected to laser microbeam microdissection (Leica Microsystems GmbH). Forty sections from each animal were used for microdissection, and microdissected samples were individually stored in 1.5 ml tubes at −80 °C until total RNA extraction.

2.4. RNA preparation, amplification and microarray analysis

Total RNA extraction from microdissected regions, quantitation of RNA yield, and RNA amplification were performed using methods described elsewhere [14,15,19].

For microarray analysis, second-round-amplified biotin-labeled antisense RNAs were subjected to hybridization with a GeneChip® Rat Genome 230 2.0 Array (Affymetrix, Inc., Santa Clara, CA).

Gene selection and normalization of expression data were performed using GeneSpring® software 7.2 (Silicon Genetics, Redwood City, CA). Per chip normalization was performed according to a method described elsewhere [14,15]. Genes with expression changes of at least 2-fold in magnitude compared with those of untreated controls were selected. Common genes with altered expression in anti-thyroid agent exposed groups were also selected.

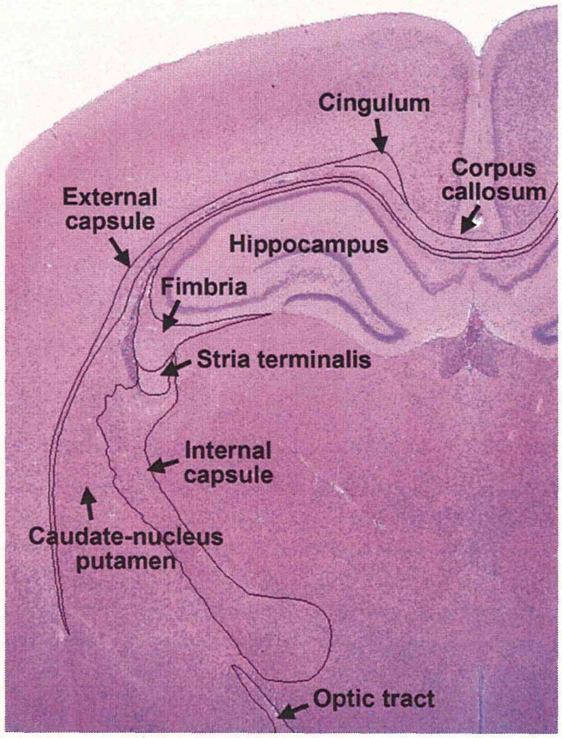

Fig. 1. Overview of the cerebral hemisphere of a male rat at PND 20 stained with hematoxylin and eosin. Magnification, 12.5×.

2.5. Real-time RT-PCR

Quantitative real-time RT-PCR using an ABI Prism 7900HT (Applied Biosystems Japan Ltd., Tokyo, Japan) was performed for confirmation of expression values obtained from microarray analysis. Selected genes showed altered expression (≥2-fold, ≤0.5-fold) in any of the anti-thyroid agent-exposed animals as compared with those of untreated controls. For example, vimentin, *Ret*, v-maf musculoaponeurotic fibrosarcoma oncogene (*v-Maf*) and tektin 4 as up-regulated genes, and *Cld11* and zinc finger homeobox 1b (*Zfhx1b*) as down-regulated ones. RT was performed using first-round antisense RNAs prepared for microarray analysis. For real-time PCR analysis, ABI Assays-on-Demand™ TaqMan® probe and primer sets from Applied Biosystems (n = 4/group) were used. For quantification of expression data, a standard curve method was applied. Expression values were normalized to glyceraldehyde 3-phosphate dehydrogenase (GAPDH) using TaqMan® Rodent GAPDH Control Reagents (Applied Biosystems Japan Ltd.).

2.6. Immunohistochemistry

To evaluate the immunohistochemical distribution of molecules identified by microarray analysis, the brains of male pups obtained at PND 20 were fixed in Bouin's solution at room temperature overnight. Ten animals for each group were used except for the untreated control group with six animals.

Antibodies against vimentin (mouse monoclonal antibody, 1:200; Millipore Corporation, Billerica, MA), glial fibrillary acidic protein (GFAP, rabbit polyclonal antibody, 1:500; Dako, Glostrup, Denmark), Ret (rabbit polyclonal antibody, 1:50; Santa Cruz Biotechnology, Inc., Santa Cruz, CA), DCC (mouse monoclonal antibody, 1:40; Leica Microsystems GmbH), and oligodendrocyte specific protein (OSP, same as Cld11, rabbit polyclonal antibody, 1:200; Novus Biologicals, Inc., Co., Littleton, CO) were used for immunohistochemistry. For antigen retrieval, sections were heated in 10 mM citrate buffer in a microwave for 10 min before incubation with anti-vimentin and -DCC antibodies. Immunodetection was carried out using a VECTASTAIN® Elite ABC kit (Vector Laboratories Inc., Burlingame, CA) with 3,3′-diaminobenzidine/H_2O_2 for the chromogen as described elsewhere [13,14]. Sections were then counterstained with hematoxylin and coverslipped for microscopic examination.

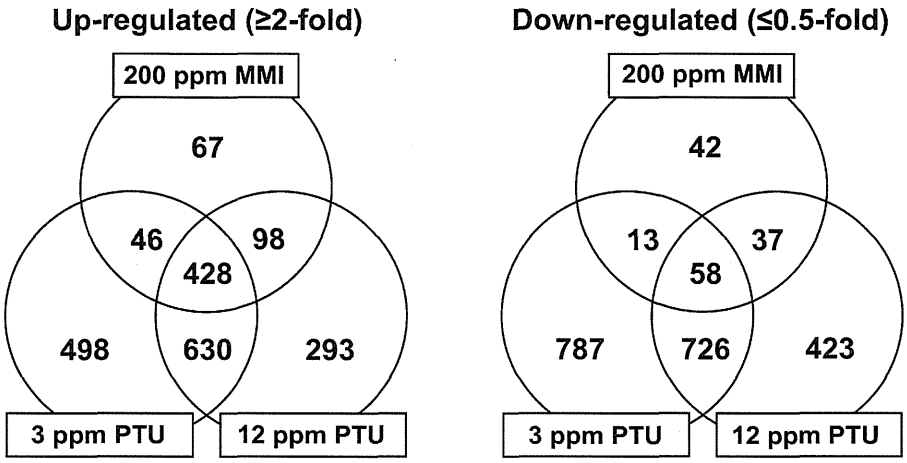

Fig. 2. Venn diagram of genes with altered expression in microarray analysis in response to maternal exposure to anti-thyroid agents. (Left) Up-regulated genes (≥2-fold). (Right) Down-regulated genes (≤0.5-fold).

2.7. Morphometry of immunolocalized cells

The number of immunoreactive cells was quantitatively measured by vimentin and Ret expression in white matter at the cingulum of the bilateral sides using two sections with an approximately 100 μm interval (i.e. four images per animal; Fig. 1), and values were normalized and expressed as those in the unit area (cm^2). GFAP-immunoreactive cells were similarly measured. For quantitative measurement of each immunoreactive cellular component containing vimentin, Ret and GFAP, digital photomicrographs at 100-fold magnification were taken using a BX51 microscope (Olympus Optical Co., Ltd., Tokyo, Japan) attached to a DP70 Digital Camera System (Olympus Optical Co.), and quantitative measurements were performed using WinROOF image analysis software 5.7 (Mitani Corp., Fukui, Japan). To evaluate immunoreactivity of DCC and Cld11 in white matter, staining intensity was scored as 0 (none), 1 (minimal), 2 (slight), 3 (moderate) and 4 (strong) by observation at 40-fold magnification.

2.8. Statistical analysis

Numerical data were assessed by one-way analysis of variance or the Kruskal–Wallis test following Bartlett's test. Statistically significant differences were analyzed by Dunnett's multiple test for comparison with that of the untreated control group. For grading immunohistochemical findings, scores of DCC and Cld11 expression were analyzed with the Mann-Whitney's *U*-test between the untreated control group and each anti-thyroid agent treated group.

3. Results

3.1. Global gene expression analysis

Fig. 2 shows the Venn diagram of genes with altered expression in microdissected cerebral white matter in treated groups in combination or individually in each treated group. Numerous common genes were found to be up- or down-regulated in two of the three treatment groups. The number of genes with up- or down-regulation in response to 3 ppm PTU was higher compared with that of 12 ppm PTU. The number of genes with

Table 1
List of representative genes associated with brain development showing up- or down-regulation common to treatments with MMI and PTU at both 3 and 12 ppm (≥2-fold, ≤0.5-fold).

Accession no.	Gene title	Symbol	MMI	PTU, 3 ppm	PTU, 12 ppm
Up-regulated (20 genes)					
NM_052803	ATPase, Cu++ transporting, alpha polypeptide	*Atp7a*	5.02	11.39	11.09
NM_001108322	T-box 1	*Tbx1*	4.20	4.34	2.31
NM_001191609	Laminin, alpha 5	*Lama5*	4.11	11.57	9.35
NM_031550	Cyclin-dependent kinase inhibitor 2A	*Cdkn2a*	3.59	2.70	3.37
NM_001114330	Glutamate receptor, metabotropic 1	*Grm1*	3.45	2.92	5.89
(NM_001114330)			(3.01)	(2.85)	(2.88)
NM_023091	gamma-Aminobutyric acid A receptor, epsilon	*Gabre*	3.20	3.91	7.46
NM_001107692	Ephrin A4	*Efna4*	3.13	5.07	6.72
NM_001002805	Complement component 4a	*C4a*	3.04	7.15	6.43
NM_019328	Nuclear receptor subfamily 4, group A, member 2	*Nr4a2*	2.97	2.87	4.92
NM_001110099	Ret proto-oncogene	*Ret*	2.89	5.01	4.39
NM_053629	Follistatin-like 3	*Fstl3*	2.85	4.28	6.08
NM_053708	Gastrulation brain homeobox 2	*Gbx2*	2.82	4.73	4.09
NM_019236	Hairy and enhancer of split 2	*Hes2*	2.76	2.93	3.11
NM_001109223	Wingless-related MMTV integration site 16	*Wnt16*	2.71	2.42	3.82
XM_001077495	Nuclear receptor co-repressor 1	*Ncor1*	2.67	2.01	2.97
NM_001012220	Cation channel, sperm associated 2	*Catsper2*	2.54	6.69	4.56
NM_001024275	Ras association (RalGDS/AF-6) domain family 4	*Rassf4*	2.31	4.67	5.43
NM_138900	Complement component 1, s subcomponent	*C1s*	2.12	3.31	3.88
NM_031140	Vimentin	*Vim*	2.11	6.01	4.27
NM_053555	Vesicle-associated membrane protein 5	*Vamp5*	2.04	2.62	3.41
Down-regulated (4 genes)					
NM_013107	Bone morphogenetic protein 6	*Bmp6*	0.23	0.38	0.25
NM_053759	Sine oculis homeobox homolog 1	*Six1*	0.45	0.35	0.46
NM_019280	Gap junction membrane channel protein alpha 5	*Gja5*	0.46	0.16	0.28
NM_133293	GATA binding protein 3	*Gata3*	0.47	0.47	0.24

Abbreviations: MMI, 2-mercapto-1-methylimidazole; PTU, 6-propyl-2-thiouracil.

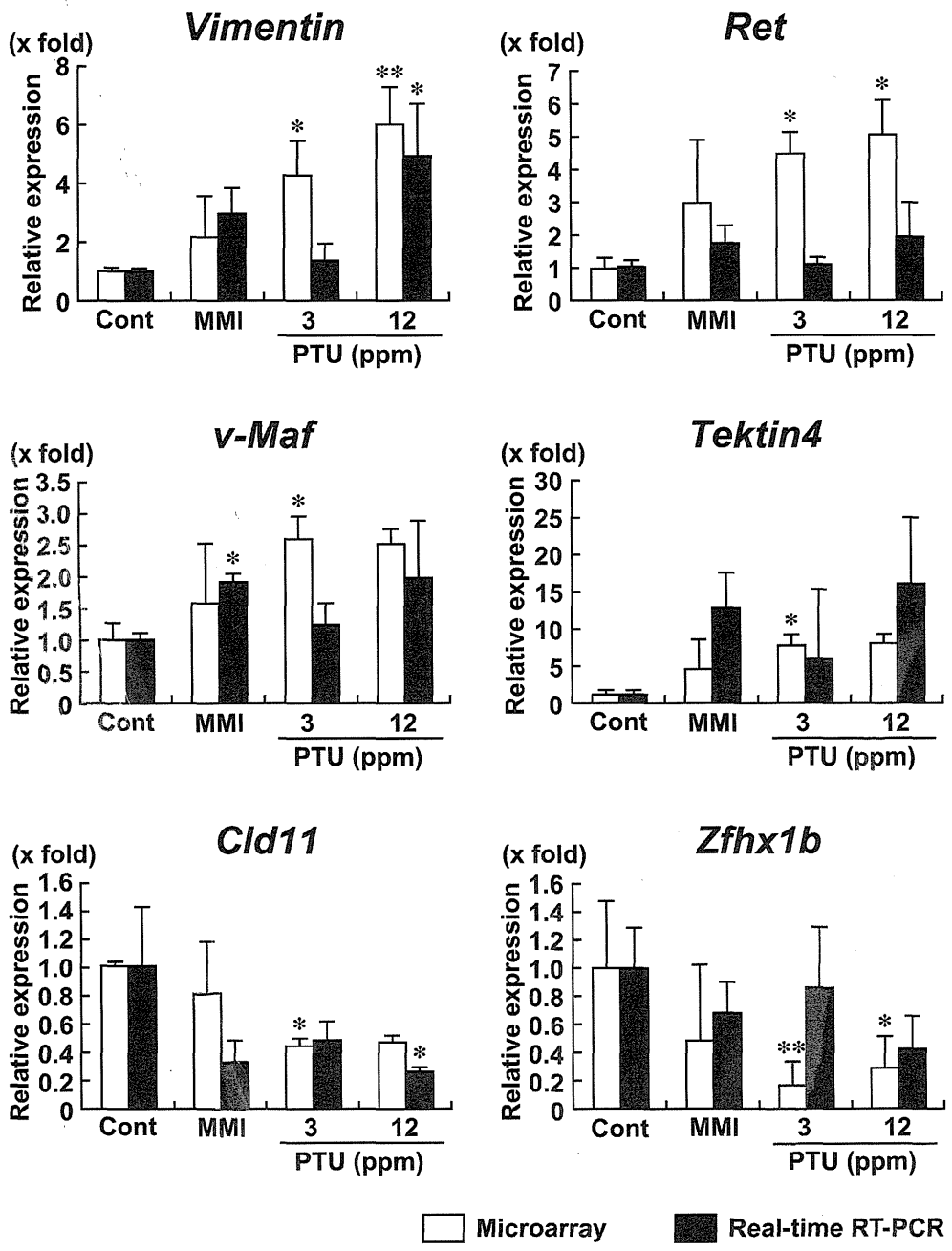

Fig. 3. Validation of mRNA expression of genes selected from microarray data ($n = 4$ in each group). $^{*}P < 0.05$, $^{**}P < 0.01$ vs. untreated controls.

up- or down-regulation in response to 200 ppm MMI was much lower compared with those of both PTU groups. Four hundred and eighty six common genes (428 up-regulated; 58 down-regulated) were identified with altered expression between MMI and both PTU groups (Fig. 2 and Supplementary data: Tables 1 and 2). Among these genes, the genes associated with central nervous system (CNS) development, cell differentiation and cell adhesion were commonly up- or down-regulated in response to anti-thyroid agents (Supplementary data: Tables 1 and 2). Twenty-four genes (20 up-regulated; 4 down-regulated) were related to CNS development involving glial cell differentiation, axon guidance, myelination, and cellular migration (Table 1). Among them, 12 up-regulated genes and two down-regulated genes showed PTU dose-dependent expression changes. For confirmation of microarray data, four genes that were up-regulated and two genes that were down-regulated in response to anti-thyroid agents were selected for mRNA expression analysis by real-time RT-PCR. Results are summarized in Fig. 3. All genes examined showed fluctuations in transcript levels in any of anti-thyroid agent treatment groups, which was similar to that of microarray data.

3.2. *Immunolocalization of selected molecules in cerebral white matter*

Immunohistochemical localization of vimentin, Ret, DCC and Cld11 was examined in the cerebral white matter. Within white

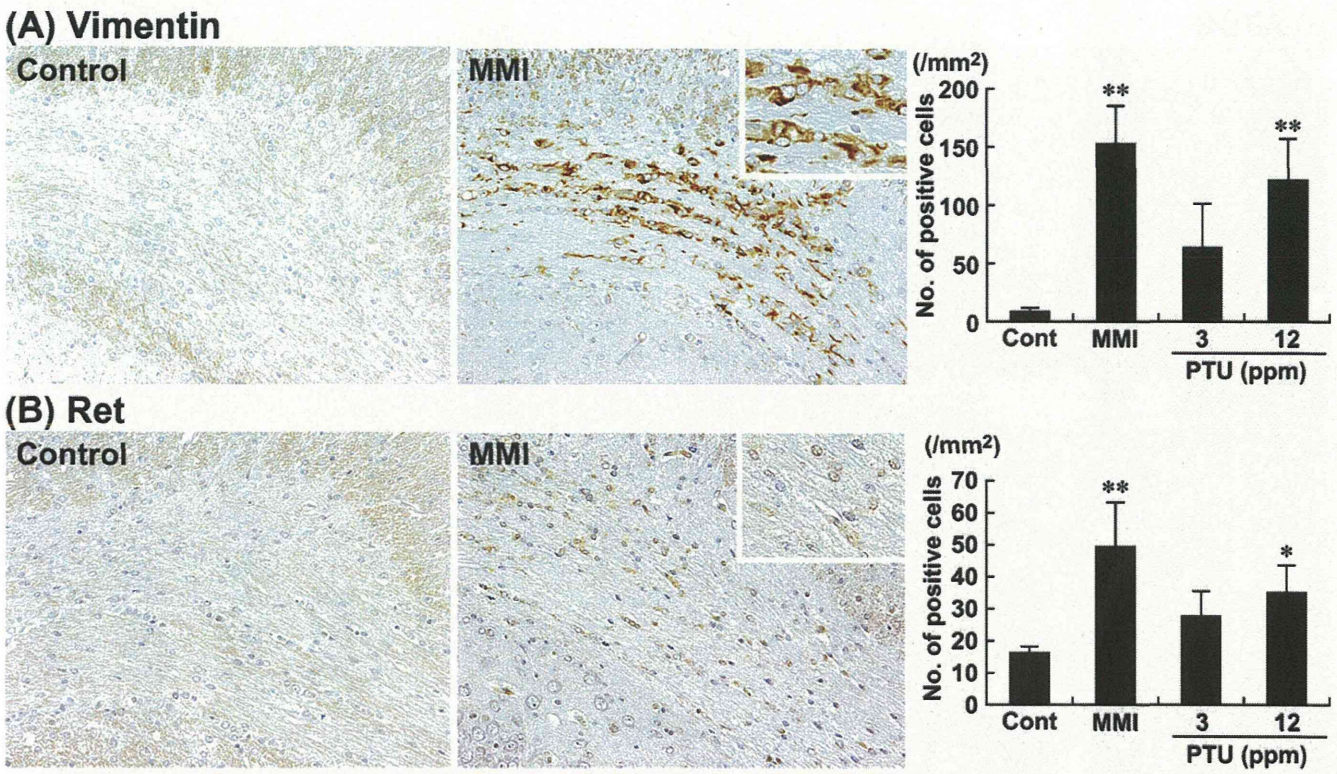

Fig. 4. Immunohistochemical distributions of vimentin- and Ret-positive cells in the while matter tissue. (A) Vimentin-immunoreactive cells in the cingulum. Untreated control animal (left) and MMI-treated animal (right). 200× magnification (inset: 400× magnification). Graph shows the mean number of positive cells within the cingulum at 200× magnification (untreated controls: $n=6$; MMI and PTU groups: $n=10$). $^{**}P<0.01$ vs. untreated controls. (B) Ret-immunoreactive cells in the cingulum. Untreated control animal (left), MMI-treated animal (right). 200× magnification (inset: 400× magnification). Graph shows the mean number of positive cells within the cingulum at 100× magnification (untreated controls: $n=6$; MMI and PTU groups: $n=10$). $^{*}P<0.05$, $^{**}P<0.01$ vs. untreated controls.

matter tissues, vimentin-immunoreactive cells were scarcely distributed in untreated control animals (Fig. 4A). After treatment with anti-thyroid agents, the distribution of vimentin-positive cells were mainly observed in the cingulum with a statistically significant increase in number with MMI and 12 ppm PTU treatments (Fig. 4A).

Ret-immunoreactive cells were mainly observed in white matter tissues of untreated control animals (Fig. 4B). After treatment with anti-thyroid agents, Ret-positive cells were mainly observed in the cingulum with a statistically significant increase in number with MMI and 12 ppm PTU treatments (Fig. 4B).

DCC showed diffuse immunoreactivity in white matter, indicating myelin sheaths with a statistically significant increase in the intensity scores of animals treated with MMI and 12 ppm PTU as compared with those of the untreated control (Fig. 5A).

Diffuse Cld11-immunoreactivity was observed in white matter, indicating myelin sheaths (Fig. 5B). The immunoreactivity showed a statistically significant increase in the intensity score of animals treated with MMI as compared with that of the untreated control (Fig. 5B).

3.3. Immunolocalization of GFAP

To investigate the cell type of vimentin-positive cells, cellular distribution of GFAP immunoreactivity was analyzed as a marker of astrocytes. Untreated control animals showed scattered distribution of GFAP-immunoreactive cells in cerebral white matter, and the number of GFAP-immunoreactive cells was higher compared with that of vimentin-positive cells. GFAP-immunoreactive cells showed a similar distribution to that of vimentin-immunoreactive cells, with accumulated distribution in the cingulum (Fig. 6). After treatment with anti-thyroid agents, the number of GFAP-positive cells was significantly increased in animals treated with MMI and 12 ppm PTU.

4. Discussion

In our previous study [16], maternal exposure to MMI and PTU induced typical hypothyroidism-related changes in the concentration of thyroid-related hormones, and variability in the distribution of hippocampal CA1 pyramidal neurons due to neuronal mismigration [16]. With regard to thyroid hormone-related changes in functions or structures in glial cell populations, gene expression alternations have been reported in myelin-related protein genes related to oligodendrocytes [20,21], as well as in enzymes or cytoskeletal components related to astrocytes [22–24]. Therefore, both oligodendrocytes and astrocytes could also be the target of developmental hypothyroidism. We, in the above-mentioned study [16], also observed changes in white matter structures with hypoplasia due to impaired oligodendroglial development as previously reported [2,9]. Using the same study samples, we, in the present study, analyzed immunohistochemical distribution of molecules that showed fluctuations in gene expression from microarray analysis of cerebral white matter tissue collected using microdissection targeting oligodendrocytes and astrocytes. This is the first report to use microarray analysis of gene expression changes induced by developmental hypothyroidism in white matter, whereas there have been such approaches for the study of cerebral cortex and hippocampal substructures [15,25,26]. We found that anti-thyroid agents caused fluctuations in a number of genes associated with CNS development involving glial cell differentiation, axon guidance, myelination, and cellular migration as listed in Table 1. Among them, vimentin, Ret, DCC and Cld11

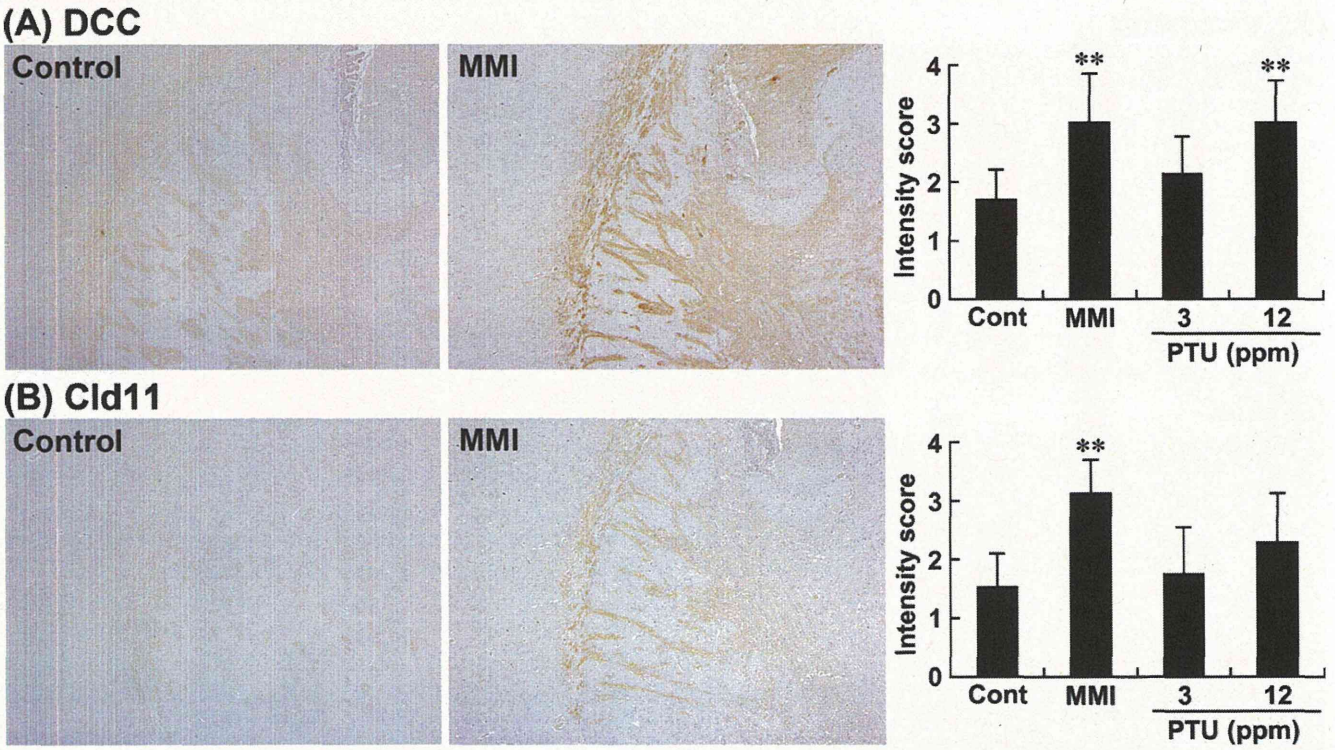

Fig. 5. Immunohistochemical distributions of DCC- and Cld11 in the while matter tissue. (A) DCC-immunoreactivity in the myelin sheath of the external capsule, internal capsule, and fimbria of the hippocampus. Untreated control animal (left), MMI-treated animal (right). 40× magnification. Graph shows the mean intensity score of immunoreactivity at 40× magnification (untreated controls: $n = 6$; MMI and PTU groups: $n = 10$). $^{**}P < 0.01$ vs. untreated controls. (B) Cld11-immunoreactivity in the myelin sheath of the external capsule, internal capsule, and fimbria of the hippocampus. Untreated control animal (left), MMI-treated animal (right). 40× magnification. Graph shows the mean intensity score of immunoreactivity at 40× magnification (untreated controls: $n = 6$; MMI and PTU groups: $n = 10$). $^{**}P < 0.01$ vs. untreated controls.

showed immunohistochemical distribution changes in the cerebral white matter of offspring after maternal exposure to PTU and MMI.

Cld11 is a four-transmembrane protein, which is primarily expressed in oligodendrocytes of the CNS and is the third most abundant CNS myelin protein [27–29]. Cld11 is involved in the formation of intramembranous tight junctions within the myelin sheath [30]. It is known that developmental hypothyroidism results in continued reduction of oligodendrocytes in the CC region from PND 10 [2]. In vitro study has shown that Cld11-overexpression results in induction of oligodendrocyte proliferation [31]. This result indicates that the overexpression of Cld11 at PND 20 is a compensatory response to decrease numbers of oligodendrocytes. However, mRNA levels were inconsistently decreased, suggesting involvement of post-transcriptional events such as those regulating mRNA stability and protein turnover.

DCC is a transmembrane receptor for netrin-1 via the fourth fibronectin type III domain [32]. Netrin-1 is a secreted protein, which elicits both attractive and repulsive responses in axonal guidance, neuronal migration and oligodendroglial migration depending on the homomeric or heteromeric combination of receptor dimers including DCC and Unc5 [33–35]. Netrin-1 signaling via DCC mediates growth cone extension and myelin sheath formation [36,37]. Therefore, increased expression of DCC in the myelin sheath at PND 20 induced by developmental hypothyroidism in the present study suggests a compensatory increase in response to suppression of myelin sheath formation [2]. However,

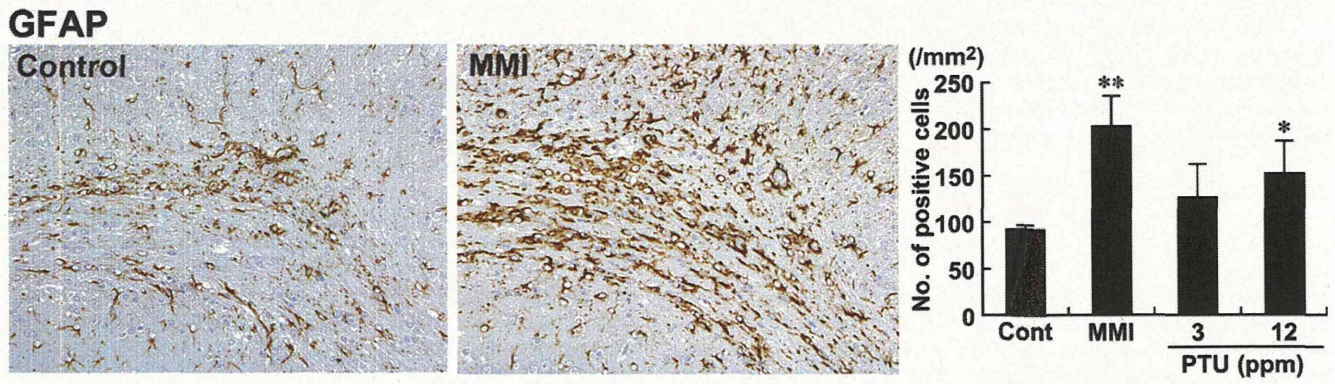

Fig. 6. Immunohistochemical distributions of GFAP-positive cells in the cingulum. Untreated control animal (left), MMI-treated animal (right). 200× magnification. Graph shows the mean number of positive cells within the cingulum at 200× magnification (untreated controls: $n = 6$; MMI and PTU groups: $n = 10$). $^{*}P < 0.05$, $^{**}P < 0.01$ vs. untreated controls.

DCC has an alternative function to drive cell death independent of both mitochondria-dependent and death receptor/caspase-8 pathways [38,39]. Moreover, DCC induces cell death in the absence of netrin-1 [40]. Because we did not find an increase in netrin-1 transcript levels using microarray analysis, it is possible that increased ligand-free DCC may lead to glial cell apoptosis. Progressive decrease in the CC area and the number of oligodendrocytes in this area during maturation after developmental hypothyroidism suggests the involvement of apoptosis due to increased ligand-free DCC [2,16].

Ret is a receptor protein–tyrosine kinase of glial cell line-derived neurotrophic factor (GDNF), a member of the transforming growth factor-β family [41]. GDNF signals play a critical role in development of the entire nervous system, kidney morphogenesis and spermatogenesis. While the functional relevance of Ret in oligodendrocytes has not been reported, this molecule is expressed in progenitor and immature oligodendrocytes in vitro and mediates cell proliferation induced by GDNF treatment [42]. Therefore, increased expression of Ret on PND 20 proceeding developmental hypothyroidism suggests a compensatory increase in response to decreased numbers of oligodendrocytes [2]. However, Ret induces cell death in the absence of its ligand similar to that of DCC [43]. Because we did not find an increase in GDNF transcript levels using microarray analysis, a progressive decrease in the size of the CC area and its oligodendrocyte density during maturation suggests involvement of apoptosis due to the increase of ligand-free Ret [2,16].

Vimentin is a member of the intermediate filament family of proteins. In the brain, this molecule is expressed in immature astrocytes during development [44–46]. Reactive astrocytes that are activated immature astrocytes during gliosis processes in response to injuries of CNS tissue also express vimentin [47,48]. Reactive astrocytes also express GFAP similar to that of mature astrocytes [47,48], suggesting that immature astrocytes can express both of vimentin and GFAP. On the other hand, developmental hypothyroidism leads to increase in vimentin expression in fetal rat brains [23]. Increase of GFAP-expression was also reported after developmental hypothyroidism in the CC region on PND 15 [49]. These results may suggest that developmental hypothyroidism increases the immature population of astrocytes. In the present study, vimentin-immunoreactive cells showed similar localization to those positive for GFAP. Therefore, a larger population of vimentin-positive cells in the cingulum induced by developmental hypothyroidism was considered to consist of immature astrocytes resembling reactive astrocytes. Interestingly, we previously reported frequent induction of subcortical band heterotopia in the CC, manifested by the appearance of aberrant cortical tissue in this anatomical area, in hypothyroid animals identical to the present study [16]. Anatomical location of this heterotopic tissue was close to the cingulum accumulating immature astrocytes, suggesting an etiological relation between the two. Alternatively, the increased immature astrocytes may simply be the reactive change in response to reduced oligodendrocytes due to developmental hypothyroidism [2,16,49]. However, developmental hypothyroidism may affect differentiation of neuronal progenitor cells, thereby inhibiting differentiation into oligodendrocytes, and instead, facilitating astrocytic differentiation during gliogenesis.

In conclusion, focusing on white matter development, we found aberrant expression of molecules associated with brain development after maternal exposure to anti-thyroid agents. Immunohistochemically, we found increased expression of Cld11, DCC, Ret and vimentin in white matter. Among them, vimentin and Ret were expressed in immature astrocytes and oligodendrocytes, respectively. Both positive cell populations were mainly distributed in the cingulum with the largest area of white matter. Because vimentin- and Ret-positive cells can be quantitatively evaluated, these molecules may be useful markers of glial cells, which respond to developmental exposure to thyroid hormone-disrupting chemicals.

Acknowledgments

We thank Tomomi Morikawa for her technical assistance in conducting the animal study. We also thank Ayako Kaneko for her technical assistance in preparing the histological specimens. This work was supported by Health and Labour Sciences Research Grants (Research on the Risk of Chemical Substances) from the Ministry of Health, Labour and Welfare of Japan. All authors disclose that there are no conflicts of interest that could inappropriately influence the outcome of the present study.

Appendix A. Supplementary data

Supplementary data associated with this article can be found, in the online version, at http://dx.doi.org/10.1016/j.reprotox.2012.03.005.

References

[1] Porterfield SP. Thyroidal dysfunction and environmental chemicals—potential impact on brain development. Environmental Health Perspectives 2000;108(Suppl. 3):433–8.
[2] Schoonover CM, Seibel MM, Jolson DM, Stack MJ, Rahman RJ, Jones SA, et al. Thyroid hormone regulates oligodendrocyte accumulation in developing rat brain white matter tracts. Endocrinology 2004;145:5013–20.
[3] Montero-Pedrazuela A, Venero C, Lavado-Autric R, Fernández-Lamo I, García-Verdugo JM, Bernal J, et al. Modulation of adult hippocampal neurogenesis by thyroid hormones: implications in depressive-like behavior. Molecular Psychiatry 2006;11:361–71.
[4] de Escobar GM, Obregón MJ, del Rey FE. Iodine deficiency and brain development in the first half of pregnancy. Public Health Nutrition 2007;10:1554–70.
[5] Comer CP, Norton S. Effects of perinatal methimazole exposure on a developmental test battery for neurobehavioral toxicity in rats. Toxicology and Applied Pharmacology 1982;63:133–41.
[6] Akaike M, Kato N, Ohno H, Kobayashi T. Hyperactivity and spatial maze learning impairment of adult rats with temporary neonatal hypothyroidism. Neurotoxicology and Teratology 1991;13:317–22.
[7] Guadaño Ferraz A, Escobar del Rey F, Morreale de Escobar G, Innocenti GM, Berbel P. The development of the anterior commissure in normal and hypothyroid rats. Brain Research Developmental Brain Research 1994;81:293–308.
[8] Lavado-Autric R, Ausó E, García-Velasco JV, Arufe Mdel C, Escobar del Rey F, Berbel P, et al. Early maternal hypothyroxinemia alters histogenesis and cerebral cortex cytoarchitecture of the progeny. Journal of Clinical Investigation 2003;111:954–7.
[9] Goodman JH, Gilbert ME. Modest thyroid hormone insufficiency during development induces a cellular malformation in the corpus callosum: a model of cortical dysplasia. Endocrinology 2007;148:2593–7.
[10] Shibutani M, Uneyama C, Miyazaki K, Toyoda K, Hirose M. Methacarn fixation: a novel tool for analysis of gene expressions in paraffin-embedded tissue specimens. Laboratory Investigation 2000;80:199–208.
[11] Uneyama C, Shibutani M, Masutomi N, Takagi H, Hirose M. Methacarn fixation for genomic DNA analysis in microdissected, paraffin-embedded tissue specimens. Journal of Histochemistry and Cytochemistry 2002;50:1237–45.
[12] Takagi H, Shibutani M, Kato N, Fujita H, Lee KY, Takigami S, et al. Microdissected region-specific gene expression analysis with methacarn-fixed, paraffin-embedded tissues by real-time RT-PCR. Journal of Histochemistry and Cytochemistry 2004;52:903–13.
[13] Shibutani M, Lee KY, Igarashi K, Woo GH, Inoue K, Nishimura T, et al. Hypothalamus region-specific global gene expression profiling in early stages of central endocrine disruption in rat neonates injected with estradiol benzoate or flutamide. Developmental Neurobiology 2007;67:253–69.
[14] Woo GH, Takahashi M, Inoue K, Fujimoto H, Igarashi K, Kanno J, et al. Cellular distributions of molecules with altered expression specific to thyroid proliferative lesions developing in a rat thyroid carcinogenesis model. Cancer Science 2009;100:617–25.
[15] Saegusa Y, Woo GH, Fujimoto H, Inoue K, Takahashi M, Hirose M, et al. Gene expression profiling and cellular distribution of molecules with altered expression in the hippocampal CA1 region after developmental exposure to anti-thyroid agents in rats. Journal of Veterinary Medical Science 2010;72:187–95.
[16] Shibutani M, Woo GH, Fujimoto H, Saegusa Y, Takahashi M, Inoue K, et al. Assessment of developmental effects of hypothyroidism in rats from in utero and lactation exposure to anti-thyroid agents. Reproductive Toxicology 2009;28:297–307.

[17] Masutomi N, Shibutani M, Takagi H, Uneyama C, Takahashi N, Hirose M. Impact of dietary exposure to methoxychlor, genistein, or diisononyl phthalate during the perinatal period on the development of the rat endocrine/reproductive systems in later life. Toxicology 2003;192:149–70.
[18] Nakamura R, Teshima R, Hachisuka A, Sato Y, Takagi K, Nakamura R, et al. Effects of developmental hypothyroidism induced by maternal administration of methimazole or propylthiouracil on the immune system of rats. International Immunopharmacology 2007;7:1630–8.
[19] Lee KY, Shibutani M, Inoue K, Kuroiwa K, U M, Woo GH, et al. Methacarn fixation—effects of tissue processing and storage conditions on detection of mRNAs and proteins in paraffin-embedded tissues. Analytical Biochemistry 2006;351:36–43.
[20] Ibarrola N, Rodríguez-Peña A. Hypothyroidism coordinately and transiently affects myelin protein gene expression in most rat brain regions during postnatal development. Brain Research 1997;752:285–93.
[21] Barradas PC, Vieira RS, De Freitas MS. Selective effect of hypothyroidism on expression of myelin markers during development. Journal of Neuroscience Research 2001;66:254–61.
[22] Farwell AP, Dubord-Tomasetti SA. Thyroid hormone regulates the expression of laminin in the developing rat cerebellum. Endocrinology 1999;140:4221–7.
[23] Evans IM, Pickard MR, Sinha AK, Leonard AJ, Sampson DC, Ekins RP. Influence of maternal hyperthyroidism in the rat on the expression of neuronal and astrocytic cytoskeletal proteins in fetal brain. Journal of Endocrinology 2002;175:597–604.
[24] Dasgupta A, Das S, Sarkar PK. Thyroid hormone promotes glutathione synthesis in astrocytes by up regulation of glutamate cysteine ligase through differential stimulation of its catalytic and modulator subunit mRNAs. Free Radical Biology and Medicine 2007;42:617–26.
[25] Royland JE, Parker JS, Gilbert ME. A genomic analysis of subclinical hypothyroidism in hippocampus and neocortex of the developing rat brain. Journal of Neuroendocrinology 2008;20:1319–38.
[26] Kobayashi K, Akune H, Sumida K, Saito K, Yoshioka T, Tsuji R. Perinatal exposure to PTU decreases expression of Arc, Homer 1, Egr 1 and Kcna 1 in the rat cerebral cortex and hippocampus. Brain Research 2009;1264:24–32.
[27] Bronstein JM, Popper P, Micevych PE, Farber DB. Isolation and characterization of a novel oligodendrocyte-specific protein. Neurology 1996;47:772–8.
[28] Bronstein JM, Micevych PE, Chen K. Oligodendrocyte-specific protein (OSP) is a major component of CNS myelin. Journal of Neuroscience Research 1997;50:713–20.
[29] Morita K, Sasaki H, Fujimoto K, Furuse M, Tsukita S. Claudin-11/OSP-based tight junctions of myelin sheaths in brain and Sertoli cells in testis. Journal of Cell Biology 1999;145:579–88.
[30] Gow A, Southwood CM, Li JS, Pariali M, Riordan GP, Brodie SE, et al. CNS myelin and sertoli cell tight junction strands are absent in Osp/claudin-11 null mice. Cell 1999;99:649–59.
[31] Tiwari-Woodruff SK, Buznikov AG, Vu TQ, Micevych PE, Chen K, Kornblum HI, et al. OSP/claudin-11 forms a complex with a novel member of the tetraspanin super family and beta1 integrin and regulates proliferation and migration of oligodendrocytes. Journal of Cell Biology 2001;153:295–305.
[32] Kruger RP, Lee J, Li W, Guan KL. Mapping netrin receptor binding reveals domains of Unc5 regulating its tyrosine phosphorylation. Journal of Neuroscience 2004;24:10826–34.
[33] Serafini T, Colamarino SA, Leonardo ED, Wang H, Beddington R, Skarnes WC, et al. Netrin-1 is required for commissural axon guidance in the developing vertebrate nervous system. Cell 1996;87:1001–14.
[34] Alcántara S, Ruiz M, De Castro F, Soriano E, Sotelo C. Netrin 1 acts as an attractive or as a repulsive cue for distinct migrating neurons during the development of the cerebellar system. Development 2000;127:1359–72.
[35] Spassky N, de Castro F, Le Bras B, Heydon K, Quéraud-LeSaux F, Bloch-Gallego E, et al. Directional guidance of oligodendroglial migration by class 3 semaphorins and netrin-1. Journal of Neuroscience 2002;22:5992–6004.
[36] Fazeli A, Dickinson SL, Hermiston ML, Tighe RV, Steen RG, Small CG, et al. Phenotype of mice lacking functional Deleted in colorectal cancer (Dcc) gene. Nature 1997;386:796–804.
[37] Rajasekharan S, Baker KA, Horn KE, Jarjour AA, Antel JP, Kennedy TE. Netrin 1 and Dcc regulate oligodendrocyte process branching and membrane extension via Fyn and RhoA. Development 2009;136:415–26.
[38] Forcet C, Ye X, Granger L, Corset V, Shin H, Bredesen DE, et al. The dependence receptor DCC (deleted in colorectal cancer) defines an alternative mechanism for caspase activation. Proceedings of the National Academy of Sciences of the United States of America 2001;98:3416–21.
[39] Furne C, Corset V, Hérincs Z, Cahuzac N, Hueber AO, Mehlen P. The dependence receptor DCC requires lipid raft localization for cell death signaling. Proceedings of the National Academy of Sciences of the United States of America 2006;103:4128–33.
[40] Mehlen P, Rabizadeh S, Snipas SJ, Assa-Munt N, Salvesen GS, Bredesen DE. The DCC gene product induces apoptosis by a mechanism requiring receptor proteolysis. Nature 1998;395:801–4.
[41] Sariola H, Saarma M. Novel functions and signalling pathways for GDNF. Journal of Cell Science 2003;116:3855–62.
[42] Strelau J, Unsicker K. GDNF family members and their receptors: expression and functions in two oligodendroglial cell lines representing distinct stages of oligodendroglial development. Glia 1999;26:291–301.
[43] Bordeaux MC, Forcet C, Granger L, Corset V, Bidaud C, Billaud M, et al. The RET proto-oncogene induces apoptosis: a novel mechanism for Hirschsprung disease. EMBO Journal 2000;19:4056–63.
[44] Pixley SK, de Vellis J. Transition between immature radial glia and mature astrocytes studied with a monoclonal antibody to vimentin. Brain Research 1984;317:201–9.
[45] Ciesielski-Treska J, Goetschy JF, Ulrich G, Aunis D. Acquisition of vimentin in astrocytes cultured from postnatal rat brain. Journal of Neurocytology 1988;17:79–86.
[46] Alonso G. Proliferation of progenitor cells in the adult rat brain correlates with the presence of vimentin-expressing astrocytes. Glia 2001;34:253–66.
[47] Pekny M, Wilhelmsson U, Bogestål YR, Pekna M. The role of astrocytes and complement system in neural plasticity. International Review of Neurobiology 2007;82:95–111.
[48] Eddleston M, Mucke L. Molecular profile of reactive astrocytes—implications for their role in neurologic disease. Neuroscience 1993;54:15–36.
[49] Sharlin DS, Bansal R, Zoeller RT. Polychlorinated biphenyls exert selective effects on cellular composition of white matter in a manner inconsistent with thyroid hormone insufficiency. Endocrinology 2006;147:846–58.

FULL PAPER *Surgery*

Pathological Classification of Canine Mammary Tumor Based on Quantifying mRNA Levels of Hormonal Receptors, SATB1, and Snail in Tissue and Fine Needle Biopsy Samples

Takahiro KOMATSU[1)], Hidetomo IWANO[2)], Masashi EBISAWA[2)], Ai WATABE[1)], Yoshifumi ENDO[1)], Kazuko HIRAYAMA[3)], Hiroyuki TANIYAMA[3)] and Tsuyoshi KADOSAWA[1)]*

[1)]*Veterinary Clinical Oncology, Department of Small Animal Clinical Sciences, School of Veterinary Medicine, Rakuno Gakuen University, Ebetsu, Hokkaido 069–8501, Japan*
[2)]*Department of Veterinary Biochemistry, School of Veterinary Medicine, Rakuno Gakuen University, Ebetsu, Hokkaido 069–8501, Japan*
[3)]*Department of Veterinary Pathology, School of Veterinary Medicine, Rakuno Gakuen University, Ebetsu, Hokkaido 069–8501, Japan*

(Received 28 September 2011/Accepted 23 December 2011/Published online in J-STAGE 10 January 2012)

ABSTRACT. Cytological diagnosis is not generally conclusive enough to identify histopathological malignancy in canine mammary tumors (CMTs). To establish cytological examination using fine needle biopsy (FNB) samples, gene expressions of hormonal receptors, human epidermal growth factor receptor 2 (HER2), and transcription regulators (Special AT-rich binding protein 1: SATB1 and Snail) were investigated in both tissue and FNB samples of CMTs. In tissue samples of malignant CMTs, especially invasive ones, low expressions of hormonal receptors and high expressions of SATB1 and Snail were detected. On discriminant analysis of tissue samples, 73.2% of CMTs were correctly classified according to histopathological examinations. In FNB samples of malignant CMTs, low expressions of hormonal receptors were detected. On discriminant analysis of FNB samples, 74.2% of CMTs were correctly classified according to histopathological examination. In conclusion, FNB gene expressions had a utility for diagnosis of CMTs malignancy in some degree. By researching more sensitive genes for malignant CMTs, the gene examination of FNB samples from CMTs will become a useful diagnostic tool that can be performed easily without anesthesia and could predict tumor malignancy and invasion prior to surgical removal.

KEY WORDS: canine, Fine Needle Biopsy, gene expression, mammary tumors.

doi: 10.1292/jvms.11-0440; *J. Vet. Med. Sci.* 74(6): 719–726, 2012

Canine mammary tumors (CMTs) are the most frequent neoplasms in female dogs. Based on the histopathological diagnosis, approximately half of CMTs is classified as malignant, and evaluation of tumor malignancy is clinically essential to determine the type of surgery [9, 17]. Histopathological diagnosis is the standard tool for determining tumor malignancy. However, most patients undergo surgical mammary gland removal without biopsy because general or local anesthesia is necessary to obtain tissue samples. On the other hand, fine needle biopsy (FNB) can be performed easily without anesthesia and is widely used to diagnose many types of tumors. However, cytological evaluation of CMTs is generally thought to be not conclusive enough to discriminate correctly between benign and malignant tumors [2]. Therefore, new cytological diagnostic tools that can be used for FNB samples are needed.

Recently, many proteins or gene expressions have been investigated for detecting tumor malignancy of CMTs. Lack of estrogen receptors (ER) and progesterone receptors (PR), which normal mammary glands should express, are well-known biomarkers associated with histologic tumor malignancy, lymph node involvement, and distant metastasis [11, 14, 26]. Moreover, in a study of ER and PR expression of 113 CMTs, lower PR expression was significantly associated with shorter survival times after surgical removal [11]. In recent years, human epidermal growth factor receptor 2 (HER2, c-erb-2) has been reported to have an important role in tumor aggressiveness. Its overexpression has been detected in 24–30% of human breast cancers [3, 30, 32]. Anti-HER2 antibody is widely used for HER2-overexpressing breast cancers as an antibody drug therapy. In the recent studies of HER2 expression of CMTs, overexpression of this protein was detected in 17.6–35.4% of malignant mammary tumors, and no or faint expression was seen in most benign mammary tumors [16, 20, 22, 25]. However, survival times and survival rates were better in dogs with HER2-overexpressing malignant mammary tumors than in dogs with tumors normally expressing HER2 [20].

These biomarkers, which are expected to be useful tools not only to classify CMTs as benign or malignant tumors but also to detect highly malignant, invasive tumors, were mainly evaluated using immunohistochemical (IHC) staining techniques. To identify gene biomarkers in CMTs, quantification of the mRNA levels of many genes, includ-

*CORRESPONDENCE TO: KADOSAWA, T., Veterinary Clinical Oncology, Department of Small Animal Clinical Sciences, School of Veterinary Medicine, Rakuno Gakuen University, Ebetsu, Hokkaido 069–8501, Japan.
e-mail: kado@rakuno.ac.jp

ing hormonal receptors and *HER2*, have been reported [21, 23, 31, 34]. In these studies, mRNA was extracted from mammary tumor tissue samples, but few reports assessed the gene expressions of biomarkers in FNB samples.

Special AT-rich binding protein 1 (SATB1) is a matrix attachment region (MAR)-binding protein and has emerged as a key factor for gene transcription. By regulating many gene expressions through remodeling chromatin architecture, SATB1 is thought to play an essential role in T cell differentiation and activation [4, 24]. Furthermore, this nuclear protein has a cage-like distribution and tethers chromatin loops to a distinct region as a genome organizer [10]. Recently, SATB1 expression has been investigated in some tumors, including human breast cancer [12, 18, 35]. Han *et al.* reported that high SATB1 expression level was correlated to a high tumor malignancy and poor prognosis in human breast cancer [18]. By reprogramming gene expression, SATB1 has been thought to make tumor cells more aggressive. Snail, which is the zinc finger transcription factor and one of the genes regulated by SATB1, has been described as a mediator of epithelial-mesenchymal transitions (EMTs) [6, 18]. EMTs are characterized by loss of cell adhesion molecules and gain of mesenchymal markers [33]. In human breast cancer, Snail was reported as an important key mediator of tumor cell invasion and metastasis by induction of EMT [7, 29]. However, the roles of SATB1 and Snail in CMTs have not been clear.

The aim of this study was to assess the utility of biomarkers for cytological examination to predict tumor malignancy and invasiveness by comparison of mRNA levels of *ER*, *PR*, *HER2*, *SATB1* and *Snail* between benign and malignant CMTs and between non-invasive and invasive CMTs, and to establish a new cytological gene examination using FNB samples.

MATERIALS AND METHODS

Patients: Fifty-five dogs studied included 14 Miniature Dachshunds, 6 Shih-Tzus, 4 Beagles, 3 each of Malteses, Papillons, and Shetland Sheepdogs, 2 each of American Cocker Spaniels, Miniature Schnauzers, Welsh Corgi Penbrakes, West Highland White Terriers, and Cavalier King Charles Spaniels, 1 each of Great Pyrenees, Poodle, Chihuahua, Japanese Spitz, and Miniature Bull Terrier, and 7 mixed breeds. These dogs had not had any malignant tumors before excisional biopsy except for the malignant mammary tumors. In 15 dogs, ovariohysterectomy (OHE) had been performed prior to the removal of CMTs. One dog with a mammary tumor was male. The dogs' mean age at the time of tumor removal was 10.0 years (range, 4 to 16 years).

Samples: Fifty-six tissue samples were obtained by excisional surgery from 55 dogs with mammary tumors. The tissue samples under 0.03 grams were obtained from the marginal tumor tissues of the specimens. The mean size of the CMTs was 2.9 cm (range, 0.5 to 11 cm). FNB samples were obtained by inserting 22-G needles into the tumors through the skin in 31 CMTs prior to tissue sample collection. After these sampling, mammary tumors were examined histopathologically by a veterinary pathologist and classified according to the WHO classification [28]. Based on the histopathological examination, the CMTs were categorized into benign or malignant, and non-invasive or invasive. Invasive tumor was defined as tumor with infiltrative growth into the surrounding normal tissues or lymph and blood vessels. All tissue or cytological samples were immersed with RNA*later* (Applied Biosystems, Foster City, CA, U.S.A.) overnight at 4°C or 30 min on ice, followed by removal of the RNA*later* and storage at −80°C.

RNA isolation and reverse transcription polymerase chain reaction (RT-PCR): Total RNA was isolated from mammary tumors using an RNeasy Mini kit (Qiagen, Hilden, Germany). DNAse digestion was performed using an RNase-Free DNase kit (Qiagen). cDNA was synthesized from 1 μg of tRNA with ReverTra Ace reverse transcriptase (Toyobo, Osaka, Japan) and oligo dT primers (Toyobo) according to the manufacturer's instructions.

Quantitative RT-PCR (qRT-PCR) analysis: cDNA that had been diluted for the amplification of the target genes (*ER*, *PR*, *HER2*, *SATB1*, and *Snail*) was used for qRT-PCR analysis. A standard curve for each gene was produced using 100- and 10-fold serial dilutions of the genes as a template (10^8, 10^6, 10^4, and 10^3 copies). The reaction was performed using a Quantitect SYBR Green PCR kit (Qiagen) and an iQ5/MyiQ Single-Color (Bio-Rad Laboratories, Hercules, CA, U.S.A.) following the manufacturer's instructions, run as triplicates of each sample. The copy number of each gene expressed in CMTs was calculated from a standard curve and normalized to that of *ribosomal protein 19 (RP19)*. Each primer sequence is shown in Table 1.

Statistical analysis: The Mann-Whitney U test was used to analyze the differences in the mRNA expression levels of target genes between benign and malignant CMTs, and between non-invasive and invasive CMTs, with $P<0.05$ considered significant. The genes that had significantly different expressions among these categories were selected for discriminant analysis. Each tumor sample was classified into these categories by discriminant analysis. The relationship between tissue and FNB samples in gene expression was analyzed by Spearman's rank correlation coefficient. Data analyses were carried out with Excel Toukei 2010 (SSRI, Tokyo, Japan).

RESULTS

Histologic study: The 56 tissue samples consisted of 28 benign CMTs (2 simple adenomas, 18 complex adenomas, 8 mixed tumors) and 28 malignant CMTs (12 simple carcinomas, 13 complex carcinomas, 1 adenocarcinoma, 1 carcinosarcoma, 1 osteosarcoma); of the malignant CMTs, 16 showed tumor invasiveness to the surrounding normal tissues or lymph and blood vessels.

Gene expressions and discriminant analysis of tissue samples: The expression level of *ER* appeared significantly higher in benign (median, 0.01; average, 0.03) CMTs than in malignant (median, 0.002; average, 0.006) CMTs. The difference in *ER* expression between non-invasive (median,